IEEE Access
Multidisciplinary ⋮ Rapid Review ⋮ Open Access Journal

Received January 6, 2022, accepted January 28, 2022, date of publication February 7, 2022, date of current version March 24, 2022.

Digital Object Identifier 10.1109/ACCESS.2022.3149588

Increasing Reliability on UAV Fading Scenarios

JOSEANNE VIANA[1,2], (Member, IEEE), JOÃO MADEIRA[2,3], NIDHI[4], (Member, IEEE), PEDRO SEBASTIÃO[1,2], (Member, IEEE), FRANCISCO CERCAS[1,2], (Senior Member, IEEE), ALBENA MIHOVSKA[4], (Member, IEEE), AND RUI DINIS[2,3], (Senior Member, IEEE)

[1]ISCTE–Instituto Universitário de Lisboa, 1649-026 Lisbon, Portugal
[2]IT–Instituto de Telecomunicações, 1049-001 Lisbon, Portugal
[3]FCT–Universidade Nova de Lisboa, 2829-516 Caparica, Portugal
[4]AU–Department of Business Development and Technology, Aarhus University, 7400 Herning, Denmark

Corresponding author: Joseanne Viana (joseanne.viana@lx.it.pt)

This work was supported by the European Union's Horizon 2020 Research and Innovation Programme through the Marie Sklodowska-Curie Project under Grant 813391.

ABSTRACT Unmanned aerial vehicles (UAVs) are the next technology to be incorporated into a telecommunications network to improve command and control on a large scale in both line-of-sight (LOS) and non-line-of-sight (NLOS) conditions. However, there is still room for improvement in terms of reliability. This paper investigates Constant Packet Combining (CPC) and Adaptive Packet Combining (APC) techniques applied to Unmanned Aerial Vehicle (UAV) communication in the presence of large-scale fading, where the channels are subject to sudden degradation for long periods due to obstructions. We use Single Carrier (SC) Frequency Domain Equalization (FDE) combined with the Iterative Block Decision-Feedback Equalizer (IB-DFE) to handle command and control messages mapped for UAV use cases. We present closed-form equations for the equalization design as well as the performance parameters such as Bit Error Rate (BER), the Packet Error Rate (PER), the throughput, the retransmissions amount, the goodput (the transmission rate without the retransmissions quantity), and the outage probability. Then, we analyze the system performance using correlated, independent, and equal channels. There is a trade-off between the overall available power, throughput, and reliability. For instance, more retransmissions result in higher reliability, power consumption and lower goodputs (effective data rates). CPC validates the transmission system and confirms the improvement of BER and PER parameters without energy efficiency optimization. APC is appealing because it can reduce the number of retransmissions for all channels used with the advantage of meeting energy efficiency requirements by adapting the overall power to the scenario experienced by the UAV.

INDEX TERMS Dynamic networks, disasters, drone simulation, packet combining, reliability, UAV, unmanned aerial vehicles, 4G, 5G.

I. INTRODUCTION

It is essential to have a reliable communication system, especially in unfortunate events, disasters, and emergencies. Hence, the environmental unpredictability and vulnerability in global systems, such as the fixed telecommunication system, has recently gained much attention among the research community in order to improve recovery and resilience mechanisms [1]. UAVs are now a part of our lives across several industries, i.e., the military, corporate logistics, gaming, and city maintenance. Studies from [2] validate UAV participation in the 5G Radio Access Network (RAN), which may improve several services, i.e., cloud, safety/proximity, best effort, high capacity, and mobility. UAV's characteristic features like low-power, low-cost, fast deployment, and Line-of-Sight (LoS) links can benefit from 5G hybrid networks and provide new services in several vertical industries [3]. Reliability is critical when a UAV experiences blind spots or blockages while being stationary or moving aerially either as a mobile base station or a relay. Moreover, transmitting and receiving status updates regarding UAVs' locations, positions and conditions under dynamic, unforeseen situations and environments periodically utilizing Command and Control (C2) Links is essential. This is the next step to ensure drone communication in the Ultra Reliable Communications paradigm for UAVs.

According to Mozzafari *et al.* [4], and Geraci *et al.* [5], three elements estimate blockage probability: the altitude of

The associate editor coordinating the review of this manuscript and approving it for publication was Miguel López-Benítez.

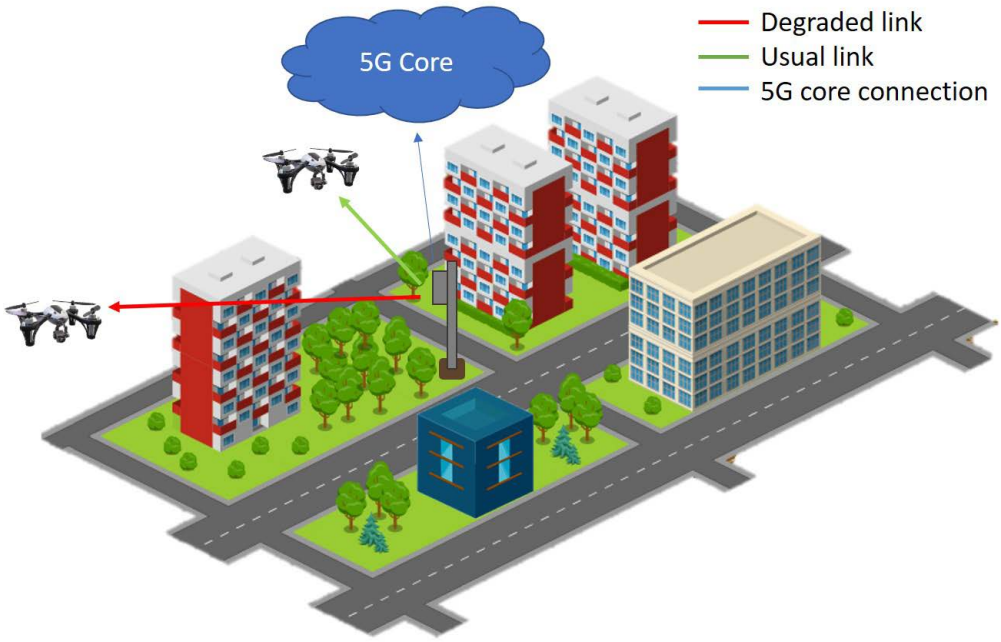

FIGURE 1. Obstruction scenario.

the UAV, the position of the obstacle sources (i.e., buildings, trees, and moving objects), and the relative position from the communication transceiver and receiver. Furthermore, there is a relationship between the high LoS links and the UAV' altitude above the ground. As the obstacle density decreases with altitude, the risk of a blockage (outage) rises inversely proportionate to the drones' height. Consequently, unblocked links are more common in Air-to-Air (A2A) connections at high altitudes than in Air-to-Ground (A2G) links. As we see with cellular communication, these blockages may produce different arrival time intervals between the first and last multipath signal components generating delay spread in drone communication. Furthermore, when the multipath fading channel has a very long path length, the different signals may be received after one symbol duration, which causes Inter-Symbol Interference (ISI). Consequently, this increases the Bit Error Rate (BER) and decreases reliability.

When the user experiences a blockage in fixed telecommunication infrastructure also referred to as a coverage hole or a weak signal zone in the telecommunication infrastructure; the instantaneous reaction is to change positions since in moving scenarios, handovers might occur. Another possibility is to wait for improvements in the channel condition and request retransmissions, which is known as the Automatic Repeat Request (ARQ) mechanism. A third option uses the modulation scheme adaptation at higher layers as this method is well adapted in the communication system.

Assuming the UAV works as aerial user equipment (AUE) connected to a terrestrial network susceptible to interference and obstacles in the environment, the UAV normally follows an optimal precalculated path to complete its mission. The European Union Aviation Safety Agency (EASA) is establishing rules and routes to limit the circulation of UAVs in the sky. Under these guidelines and circumstances, there might be situations where the UAV has poor connection and it cannot change the predefined path in the system to a new one that takes into account the signal strength. Furthermore, objects like trees and barriers are inevitable as the city is in constant transformation. Also, timing is critical in unfortunate circumstances. Therefore, ideally, blockages should not limit UAV operations, either increasing decision-making delays at higher layers or increasing the intermittent UAV connection between two or more smallcells using the Reference Signal Received Power (RSRP) known as handover burn.

According to the definition, reliability means guaranteeing that the transmission BER is lower than 10^{-4}; in other words, users receive 99.0% or more of the forwarded messages. On the other hand, unreliable communication indicates that several channel realizations do not support the transmission rate T. Unfortunately, reliability draws limited attention in the research community, where trajectory optimization and increasing coverage seem to be in the spotlight. Usually, there is a trade-off between the data rate, energy, and reliable communications. Therefore, we explore both network characteristics and discover an optimal trade-off mechanism that is applicable to UAV scenarios. This mechanism adjusts the required power according to the surrounding environment using the information obtained from NACK packets after the retransmission attempt, saving resources by avoiding unsuccessful packet transmission on a continuous basis.

A. RELATED WORK

Most of the work on reliability issues proposes an arrangement between terrestrial and aerial links or optimizes interference, packet sizes, and non payload packets in the

control plane, the channel model, and its derivations. For example, in paper [6], the solution to increase reliability was interference management and antenna beam selection. Ming-min *et al.* [7] demonstrates that reliability is proportional to the data rate and accessible energy. The author from [8] establishes reliability criteria that takes into account the minimum amount of links between drones to assure connectivity in failure scenarios. She *et al.* [9] suggests an algorithm for control and non payload packets in the URLLC scenarios. Alef *et al.* [10] derives a mathematical model message delay distribution between vehicles and road-side-units. In [11], the author contribute to a framework to increase reliability in UAVs considering small-scale fading. Han *et al.* [12] proposes a two-step protocol using D2D communications for UAV swarm scenarios. Also, the author of [13] provides some insights about reliability with respect to UAV heights presenting an experimental study where latency was measured in term of reliability e.g expecting packet arrival. Shafique *et al.* [14] evaluates a transmission-reception system using ARQ retransmission and explains several topics in channel modelling including: frame structure, channel modeling, UAV relay analysis, cooperation schemes, and diversity techniques.

In terms of channel modeling, Bithas *et al.* [15] suggests a channel model for drone communications. In [16], a way to improve channel estimation using golden sequences is introduced. Kumari *et al.* [17] describes a way to equalize the channel and the carrier frequency offset using Deep learning techniques. Ji *et al.* [18] uses multiple relay energy harvesting schemes to control large-scale fading in drone scenarios. Khuwaja *et al.* [19] describes the outage probability as a function of user mobility, propagation environment, and channel fading models in UAV scenarios. Ernest *et al.* [20] uses Non-Orthogonal Multiple Access (NOMA) to estimate performance in UAV communication systems over Rician fading channels. In [21] a trajectory optimization in Rician fading channels for data harvesting is proposed. Cui *et al.* [22] presents measurements for Air-to-Ground (A2G) channels across several frequencies. Liu *et al.* [23] characterizes and develops a model for UAV Air-to-Air (A2A) channels with Low-Altitude based on field measurements. The authors from [24] define a model for high-altitude fixed-wing UAV A2G channel communications between aerial base stations. Wang *et al.* [25] suggests coverage optimization considering small-scale and large-scale fading channels. Pereira [26] analyzes packet combining techniques using SC-FDE in terrestrial networks. We propose a different approach mixing reliability with a power controlled mechanism using CPC and APC techniques.

B. NOTATIONS AND DEFINITIONS

Lower-case letters ($a, b, \ldots$) denote scalar variables, boldface lower-case letters ($\mathbf{a}, \mathbf{c}, \ldots$) represent vectors, and boldface capitals (A, B, ...) correspond to matrices. Furthermore, lower case letters express time-domain variables and upper case letters indicate frequency-domain letters; Next, $\tilde{x}$, $\hat{x}$ and $\bar{x}$ represent sample estimates, ''hard decision'' estimates, and ''soft decision'' estimates of x, respectively.

TABLE 1. Abbreviation list.

Abbreviation	Definition
CPC	Constant Packet Combining
APC	Adaptive Packet Combining
UAV	Unmanned Aerial Vehicle
SC	Single Carrier
FDE	Frequency Domain Equalization
IB-DFE	Iterative Block Decision- Feedback Equalizer
D2X	Drone-to-Everything
BER	Bit Error Rate
PER	Packet Error Rate
RAN	Radio Access Network
LoS	Non Line of Sight
NLoS	Line of Sight
C2	Command and Control
A2A	Air to Air
A2G	Air to ground
URLLC	Ultra Reliable Low Latency Communications
ARQ	Automatic Repeat Request
AUE	Aerial User Equipment
RSRP	Reference Signal Received Power
NOMA	Non-Orthogonal Multiple Access
OFDM	Orthogonal Frequency Division Multiplexing
SNR	Signal to Noise Ratio
IC	Independent Channels
CC	Correlated Channels
EC	Equal Channels
FFT	Fast Fourier Transform
IFFT	Inverse Fast Fourier Transform
ISI	Intersymbolic Interference
NACK	Negative Acknowledgement
DFT	Discrete Fourier Transform
QPSK	Quadrature Phase Shift keying

C. MOTIVATION AND CONTRIBUTIONS

This paper studies the combination of Constant Packet Combining (CPC) and Adaptive Packet Combining (APC) with the Iterative Block Decision Feedback Equalizer (IB-DFE) and its application to UAV physical layer communications. Additionally, we add Markov chains to simulate blocking situations that may occur in the environment. Finally, we use

the SC-FDE technique for transmission, which is advantageous in drone scenarios, as it is more energy-efficient than the Orthogonal Frequency Division Multiplexing (OFDM) technique.

This paper aims to contribute to:

- The analysis of CPC and APC techniques applied to UAVs when the drone's LoS with the base station is restricted. The proposed method reduces the number of unsuccessfully transmitted blocks when the drone experiences fading due to obstacles and barriers. Furthermore, as the transmission/reception system works in the physical layer, and the number of calculated DFTs is the same as the mechanism adopted in terrestrial communications, CPC and APC techniques could be used in real-time scenarios;
- The design of equalization parameters to process transmitted signals;
- The comparison of linear and non-linear equalization schemes where CPC and APC are applied to independent, correlated, and equal channels in UAV settings;
- The closed form equations for the design of equalization parameters, the BER, the PER, outages, as well as throughput in the physical layer;
- The use of signal processing methods to cope with a variety of channel types: independent, correlated, and equal;

The remaining paper is organized as follows: Section II presents the system model. It discusses channels, Markov chain implementation and introduces the theoretical design of the linear and non-linear equalization for CPC and APC usability. Section III explains the system metrics related to performance derived from the simulation. The results of the performance evaluation are presented in Section IV, along with an explanation of them. Finally, Section V concludes this paper.

II. SYSTEM MODEL

The experiment simulates a drone trajectory with constant speed, where obstructions are added in the middle of the path forcing the drone to change direction towards a restrictive communication condition. This circumstance, typically, compromises the link between the UAV and the base station resulting in an unreliable connection. The base station is located at a fixed position (x_b, y_b, z_b) as illustrated in figure 1.

First, we characterize the communication connection between the UAV and the base station. We employ three distinct kinds of complex band channels, denoted by the terms uncorrelated, equal, and correlated to transmit blocks $\{X_k; k = 0, 1, \ldots, N-1\}$ in the frequency domain. Next, we detail the power probability applied to the channel to simulate the obstacles in the scenario. Finally, we deduce the mathematical formulation related to the equalization design and the techniques utilized to change the re-transmissions model.

Considering the channels encountered by wireless devices, uncorrelated channels (independent) perform better. They create a completely new channel after the coherence time and because of that there is a better chance to send the packet successfully than a correlated channel or even the same channel, mainly if the channel is compromised. Although, the channel may remain the same in some instances in the UAV scenarios, using uncorrelated channels between the retransmission attempts might improve performance as we see in wireless communication.

In the proposed experiment, when the system detects a sudden decrease in power at the receiver, it immediately retransmits the block and combines the energy of the lost block with the energy of the re-transmitted one, therefore applying a packet diversity strategy.

For UAVs, the worst-case scenario is duplicating the energy related to the block even though we might have a rejected block. However, the successive retransmissions may contribute to decreases in the effective PER. Additionally, the system can send feedback about changes in the available power to the transmitter to increase the power between retransmission attempts. This last feature improves the goodput rates by reducing the number of retransmission attempts.

A. THE COMMUNICATION LINKS

In the system, the propagation channel that interconnects the terrestrial BSs and UAVs is the linear, multi-path continuous-time complex baseband (tap) channel. Equation (1) calculates the frequency response of the specific channel:

$$H_k(f) = \sum_{l=1}^{L} \zeta_l \exp(-j2f\pi\tau_l) \tag{1}$$

where f is the frequency band and ζ_l^L and τ_l^L are the multipath ray's l_{th} attenuation and the propagation delay, respectively. The system adopts the Rician model in which one of the multipath rays is not susceptible to any loss, and other independent rays can be characterized using Gaussian random variables with a zero mean and a variance of (σ^2_{NLoS}) identically distributed. Without loss of generality, the distance of both devices can be calculated using the 3D Euclidean distance $||d_{bs} - d_{uav}||_2$ equation.

The Independent (IC), Correlated (CC), and Equal (EC) channels' characteristics employed between retransmission attempts in the simulation depend on the multipath factor α. As a result, by including this factor in equation (1), just as we did in equation (9), we may examine the total influence on channels adopted in the point-to-point link.

$$H_k^R(f) = \sum_{i=1}^{N_{rays}} \alpha_i(\tau) + \zeta_{l,d} \exp(-j2f\pi\tau_l) \tag{2}$$

N_{rays} is the amount of multipath components in the simulation. In the IC experiment, all channels use independent slots for each retransmission attempt. Equation (3) describes the IC α parameters.

$$\sum_{i=R} \alpha_i(\tau) \neq \sum_{i=R+1} \alpha_i(\tau) \tag{3}$$

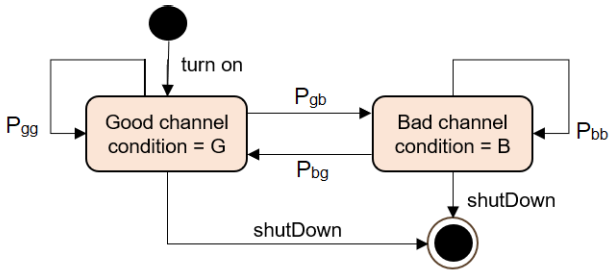

FIGURE 2. Markov chain for channel probability.

Following the same notation, we characterize the correlated channels by applying the equation: (4):

$$\sum_{i=R} \alpha_i(\tau) = \sum_{i=R+1} \alpha_i(t)\phi + \epsilon \tag{4}$$

where ϕ represents the channel correlation between slots and $(1 - \phi^2)(\alpha_i^2)$ provides the variance of the correlated channel and ϵ is the error from the Gaussian model. In EC scenarios, channels use the same multipath configuration for each retransmission attempt as equation (5) depicts.

$$\sum_{i=R} \alpha_i(\tau) = \sum_{i=R+1} \alpha_i(\tau) \tag{5}$$

The results of the retransmission summation depend on the characteristics of the channel throughout each retransmission attempt and the channel characteristics (e.g independent, correlated, and equal) depend on the multipath factor.

B. MARKOV CHAINS FOR CHANNEL PROBABILITY

Using discrete Markov Chain Probability, it is possible to add some randomness in the channel power during the simulation emulating obstacles in the environment. Therefore, we create two different states in the channel that we specify as good and bad, which are G and B, respectively. Equation (6) presents the transition probability. Equations (7) and (8) present the good and bad state probabilities, correspondingly. Figure 2 illustrates the state transition diagram that represents the Markov chain for the channel condition. When the simulation begins, a random variable determines the channel probability for both the initial states and the subsequent transitions to those states.

$$\mathbf{U} = \begin{bmatrix} P_{gg} & P_{gb} \\ P_{bg} & P_{bb} \end{bmatrix}. \tag{6}$$

$$P_G = P_{gg} + P_{bg} \tag{7}$$

$$P_B = P_{bb} + P_{gb} \tag{8}$$

We define the Urban factor *Urb* variable as the percentage of blockage experienced by the UAV that means NLOS connections (in a bad state) during the simulation.

Figure 3 depicts an example of sudden power changes in the receiver due to obstructions while using independent channels. There are four distance intervals where the power decreases abruptly i.e., 0-4m, 6-14m, 18-26m, and

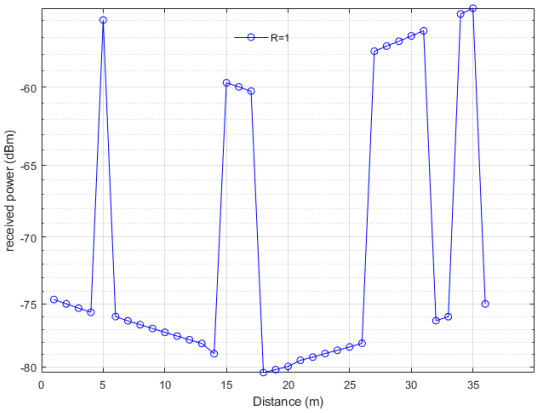

FIGURE 3. Received power changes due to obstructions in the scenario over time.

32-33m. The power variation simulates objects in the trajectory according to the probability the Markov chains define. Before and after these periods, power changes according to the corresponding path loss in the distance between the drones and the base station.

The frequency domain channel with all the elements is presented in equation:

$$H_k^R(f) = P_{state} \sum_{i=1}^{N_{rays}} \alpha_i(\tau) + \zeta_{l,d} \exp(-j2f\pi\tau_l) \tag{9}$$

where P_{state} is the good or bad channel probability defined by the Markov chain (depending on the LoS or NLoS connection avalability), α is the multipath factor that specifies the channel type between the retransmission attempts.

C. EQUALIZATION AND PACKET COMBINING

Figure 4 depicts the receiver's block diagram, including linear and non linear IB-DFE equalization blocks, and both CPC and APC techniques. When a block is not successfully received, the system tries to recover the packet using a five-step solution as the following describes:

1) The receiver attempts to recover data employing IB-DFE;
2) The receiver instantly requests retransmission;
3) The receiver notifies the transmitter about the power needed to retransmit the block (APC);
4) The receiver combines the energy of the defective block with its retransmitted block (linear scheme);
5) The transmitter increases the transmission power for the next packet (CPC and APC).

In Single Carrier Block Transmission Schemes (SC-FDE), the Fast Fourier Transform (FFT), and the Inverse Fast-Fourier Transform (IFFT) data block conversions $x_n; n = 0, 1, \ldots, N-1$ are done on the receiver side which reduces signal processing in the transmitter. This makes it an option for uplink transmissions. After the decision block, the equalization minimizes the ISI impact related to

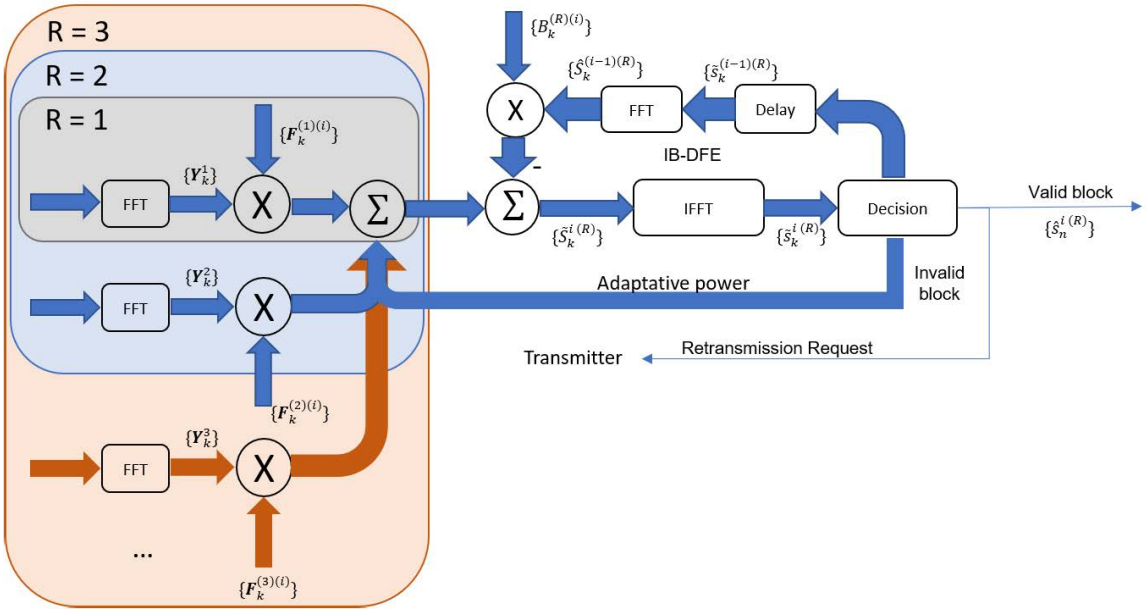

FIGURE 4. Detailed blocks reception with the combining technique.

the delay spread in the transmitted symbols using linear or nonlinear schemes. With linear packet combining, if the transmitted block is still invalid after the equalization procedure, we keep the energy ϕ_k associated with the rejected block in the receiver's memory and immediately add the energy of that block to the energy of the retransmitted one.

In CPC and APC, in addition to the features that linear packet combining provides, the receiver also sends power information from the previous valid received packet as feedback to the transmitter to adjust the power of the next retransmission. The end result reduces the number of necessary retransmissions, increases goodput rates, and the transmitted power may be optimized. Power information is potentially available in Negative Acknowledgment (NACK) packets in the transmitter.

In these simulations, the analysis of retransmission procedures takes place at the physical layer.

The system design begins with the frequency response of the receiver signal after each retransmission without obtaining any adjustment according to equation (10):

$$Y^R_{(k,d)} = H^R_{(k,d)} X^R_k + N \tag{10}$$

where X^R_k is the Discrete Fourier Transform (DFT) of the transmitted signal x^R_k, R is the retransmission attempt, and $N \sim \mathcal{CN}(0, \sigma^2_k)$ is the noise in the channel, while k is an available frequency in the bandwidth.

Our strategy uses the energy received by the successfully transmitted packets between the UAV and the base station to estimate the energy difference while the UAV passes an obstacle. Equation (11) presents the comparison factor used to estimate the power between retransmissions.

$$\phi^R_k = \frac{\sum_{r=2}^{R} |h_r(\tau)|^2}{\sum_{r=1}^{R-1} |h_r(\tau)|^2} \tag{11}$$

where r is the current transmission attempt and the h_r is the respective channel.

Equation (12) highlights the impact of the adaptation factor ϕ^R_k in the received power after each retransmission attempt:

$$Y^{R+1}_{(k,d)} = H^R_{(k,d)} \phi^R_k X^R_k + N \tag{12}$$

The total number of transmitted packets P is defined as $R + 1$. In the three mechanisms (linear, CPC, and APC), the first transmission attempt configures $\phi^1_k = 1$, which indicates that the reception power after retransmission will alter according to the comparison factor that the combiner block estimates in order to improve the reception quality [27].

The matrix multiplication for the reception illustrated in (12) for one frequency $k = 1$ implies that the factor ϕ^1_k is a diagonal matrix and where the main diagonal contains the retransmission comparison factor $diag(|\phi^1_1|^2), \ldots, |\phi^R_1|^2)$.

1) LINEAR EQUALIZATION

By default, SC-FDE employs linear frequency domain equalization to process the symbols available on the receiver side. Equation (13) defines the output samples of the linear FDE block after R retransmission attempts.

$$\hat{X}^{(R)}_k = \sum_{r=1}^{R} F^R_k Y^R_{(k,d)} \tag{13}$$

where the parameter $F^{(i,R)}_k$ represents the feedforward coefficient in both linear and non linear equalization, and $Y^R_{(k,d)}$ represents the received power in equation (10). The system employs the Mean Square Error (MSE) from (15) to estimate the received symbol as follows:

$$MSE = \frac{1}{N_2} \sum_{i=1}^{N-1} E[|\hat{X}^{(R)}_k - X^{(R)}_k|^2] \tag{14}$$

$$= E[|{F_1}^T Y_1^R - X_1^R|^2] \tag{15}$$

Next, we utilize the Lagrangian multiplier to generalize the F_k parameter by minimizing the MSE for each k during the retransmission attempt as in (16):

$${F_k}^{(i)} = \frac{H_{(k,d)}^R(\phi_k^R)}{(H_k)^2(\phi_k^R)^2(1-\rho^{2(i-1)}) + \frac{(\sigma_N)^2}{(\sigma_s)^2}} \tag{16}$$

where $\rho = \mathrm{E}[{X_k}^{(i-1)} X_k^*]/E[|X_k|^2]$ is the correlation factor between the previously estimated symbol and the current iteration and $(\sigma_N)^2/(\sigma_s)^2$ is the reciprocal of the SNR.

2) NON-LINEAR EQUALIZATION

In non-linear equalization, the system tries to estimate the symbol recursively according to feedback estimation. Two elements define the IB-DFE design, the F_k parameter which is analogous to the linear case and the feedback parameter B_k. After each retransmission, IB-DFE estimates the received symbol in each iteration reducing the ISI and improving the overall system performance in the process.

Equation (17) depicts the detected symbol after IB-DFE according to the received signal using hard decision symbol estimates.

$$\hat{X}_k^{(R)} = \sum_{r=1}^{R} \sum_{i=1}^{I} F_k^{(i,R)} Y_k^R - B_k^{(i,R)} \hat{X}_k^{(i-1)(R)} \tag{17}$$

Non-linear equalizers use feedforward (F_k) and feedback (B_k) parameters to estimate the ISI interference of the detected symbol $\hat{X}_k$ and subtract it in the next iteration of the equalization.

With the help of the MSE criterion and Lagrangian multipliers, it is feasible to estimate the new values for Fk and Bk, assuming that the transmission of one frequency is k.

We define the MSE in each IB-DFE iteration as:

$$MSE = E[|{F_1}^T Y_1^R - B_1 \bar{X}_1^R - X_1^R|^2] \tag{18}$$

The F_k parameter is the same in equation (16) Next, we estimate the equation for B_k:

$${B_k}^{(i)} = {F_k}^R H_{(k,d)}^R \phi_k^R \tag{19}$$

where ϕ_k^R is the adaptation factor. Analyzing the F_k matrix size in equation (16), it is clear that the matrix order increases according to the number of retransmissions ($R \times R$), which is not computationally practical. Authors from [28], and [29] demonstrate that it is possible to reduce the matrix order from $R \times R$ to $C \times C$ where $C \ll R$ by associating the matrix $[IA - BD]$ with its inverse MM^{-1} in both ways $M^{-1}M$. The result of the proposed matrix is $D^{-1}B(I + AD^{-1}B)^{-1}$. Equation (20) depicts the method in (16):

$$F_k^{(R)} = \sqrt{\phi_k^{*(R)}} \left(\frac{\sigma_N^2}{\sigma_X^2} + H_{(k,d)}^{T(R)} \phi_k^R H_{(k,d)}^{*(R)} \right)^{-1} \tag{20}$$

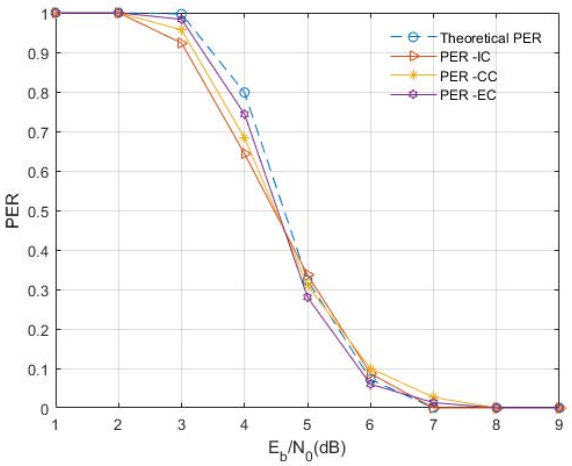

FIGURE 5. PER estimation based on BER results for all channels, R = 1.

III. SYSTEM METRICS

Using the MSE equation from (15), we derive the BER formula for each retransmission using fitting techniques.

$$TheoreticalBER_R = Q(MSE^{-\frac{1}{2}R}) \tag{21}$$

Next, we deduce the PER for each retransmission attempt using fitting techniques for all channels as figure 5 illustrates:

$$TheoreticalPER_R = 1 - (1 - BER_R)^N \tag{22}$$

where N is the FFT size.

When the minimum required SNR is unachievable due to drone distance or the diffraction effects of the obstacles, we immediately ask for retransmissions. The equation for retransmission attempts for the scenario in this paper is:

$$Retr_d = (PER * P_{tot}) - P_{out} \tag{23}$$

where P_{tot} is the total received packets. The linear adaptation system obtains the outage probability P_{out} through estimating the amount of unsuccessful packages after N number of retransmission attempts of the drone's positions in critical locations.

We could keep trying to transmit the blocks until there were no errors. Nevertheless, in practice, if we fail after R attempts, we need to change the transmission parameters (i.e., transmission power, carrier frequency, or the base station, etc.) since the channel is excessively defective. In other words, if the power in the receiver is less than the threshold after summing all the retransmissions, we assume that the block won't be received. Consequently, transmission is suspended.

Therefore, equation (26) defines the P_{out} of the terminal node when P_{thr} is the threshold.

$$P_{ret-total} = \phi_{k_1} Y_1 + \phi_{k_2} Y_2 + \phi_{k_3} Y_3 \ldots. \tag{24}$$

$$= \sum_{r=1}^{R} \phi_{k_r} Y_r \tag{25}$$

$$P_{out} = P_{thr} > P_{ret-total} \tag{26}$$

TABLE 2. Key configuration parameters.

General Parameters	Values
Modulation	QPSK
Equalization Scheme	IB-DFE
DFT-size	N = 1024 symbols
Data lenght	B = 100
Channel Correlation	θ = 0.1-0.8
Realizations non-linear IB-DFE	Iter = 5
Number of rays	L = 16 rays
Distance base-station UAV	d = 10-100
UAV height	H = 10-50
Maximum retransmission attempts	R = 4
Urban factor	Urb = 10% 60% 50%

where Y represents the received power and $P_{ret-total}$ increases or decreases linearly: We could model the increase of power ϕ_k^r in CPC and APC using the power series, but in practice it is not feasible for high values.

In this scenario, we calculate the throughput T including only successful package receptions and its basis is PER:

$$T = (1 - PER)bits \tag{27}$$

where *bits* is the amount of data transmitted over time. In addition, the equation 30 estimates the delay amongst the initial and the final required transmission attempt to attain optimal power in the linear case without power adaptation:

$$delay = 1 + \sum_{r=1}^{R} pTs \tag{28}$$

where p refers to the amount of retransmitted packets required to achieve the optimal power and *Ts* in the block delay and the cumulative probability distribution (CDF) on the reveived power over the retransmission attempts in the UAV can be written as:

$$Pr(P_{ret-total} < P_{opt-power}) = \sum_{r=1}^{R} P_{(ret-total)(k)} \tag{29}$$

IV. RESULTS AND DISCUSSION

Below we discuss the results of the proposed systems. First, we consider the linear adaptation. Next, we cover the constant adaptation factor ϕ_k^R, followed by a discussion about the outcomes of dynamic adaptation in response to channel fluctuations.

The channels used in the simulation were the continuous-time complex base-band (tap) channels described in section II regarding equal, correlated, and independent properties between the slots. We used the Quadrature Phase Shift Keying (QPSK) modulation scheme as well as SC-FDE with Linear and Non-Linear Equalization (IB-DFE). The results were obtained using Monte Carlo simulations.

We increased values for the SNR at the transmitter during the simulation. The transmission data length was $B = 100$, and R represented the maximum number of transmissions allowed for each block. As UAVs have limited power, we configured the maximum achievable gain as 20 depending on the scenario. The amount of IB-DFE iterations was $Iter = 5$. The Urban Factor refers to the percentage of obstacles per total area configured in the simulations, For the linear equalization Urb = 10%, for the CPC the configured value was 60% and for the APC the value was 50%. The key configuration parameters are described in table 2.

In the linear adaptation system, the energy of the retransmitted packets was added to the receiver to increase the overall power reception. CPC and APC transmission schemes included the linear adaptation feature and extended it using feedback mechanisms to send information to the transmitter about the minimum power required so it could be adjusted before losing more data.

It used the energy from previous successful blocks and channels to establish the ratio gain. Although we generated random obstacles in the simulation, for the sake of simplicity, we assumed that the sudden slow fading loss was the same for all of the channels.

The signal received overtime was estimated using equation (30):

$$y_{uav}(t, p)_r = h(t, p)_r * x(t)_r + n(t)_r \tag{30}$$

where $x(t)_r$ is the transmitted signal. $n(t)_r$ is the noise associated with the retransmission parameter r. $h(t, p)$ represents the channel in the time domain described in equation (1) as a function of the distance between the drone and the base station.

A. LINEAR EQUALIZATION WITHOUT POWER ADAPTATION

In the linear Adaptive transmission, the energy from each retransmission boosted the total reception power. Taking as an example, the figure 6 depicts how the total energy rose after four retransmission attempts across all channels. As a result, we can see that the overall power during fading (between 20 and 24m and 26m) rose four times between the first and final retransmissions (R = 1 and R = 4), respectively.

Figure 7 and Figure 8 depicts the BER and PER vs the normalized SNR Eb/N_0 per retransmission attempt (R) for each channel (IC, CC, EC) respectively. According to the results in BER, independent channels showed the most significant improvements over the course of four retransmission attempts. They recovered very fast after fading. For example, when comparing the first and second retransmissions, the Eb/N_0 improved from roughly 26 dB to 23 dB when the packet loss was 10^{-3}. This gain was related to the uncorrelation between the blocks in the slot and the Rician channel model utilized in the simulation.

Figure 9 shows the retransmission amount (R1, R2, R3, R4) for each channel (IC, CC, EC) during fading, specifically

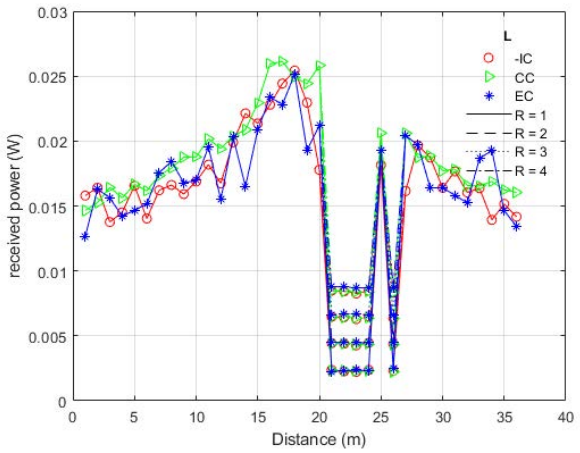

FIGURE 6. Recovered signal after adaptive packet combining in the second retransmission.

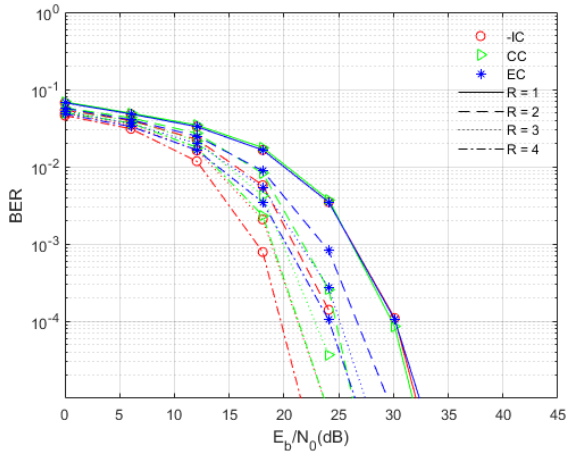

FIGURE 7. BER - IC, CC, EC channels vs Eb/N_0 over all distances.

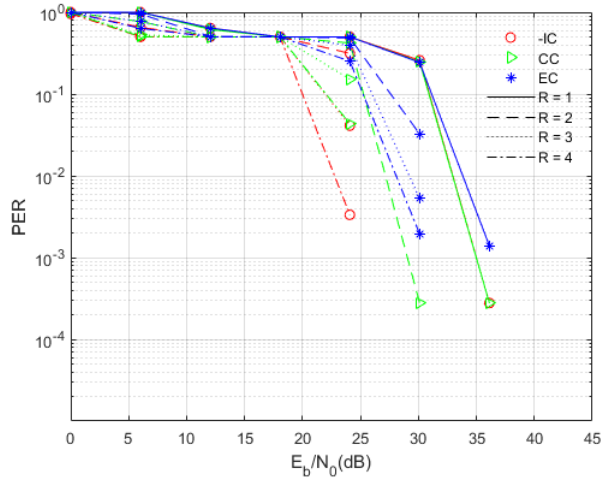

FIGURE 8. PER - IC, CC, EC channels respectively vs Eb/N_0 over all distances.

in the range between 20m and 24m and at 26m. As a result of fading, when the UAV lost packets while passing over obstacles and barriers, the number of retransmissions increased.

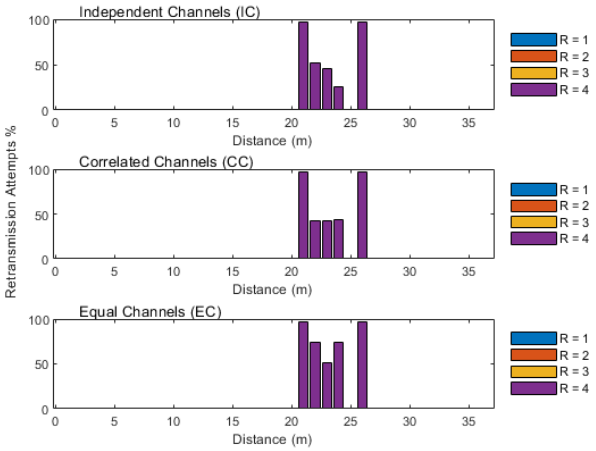

FIGURE 9. Retransmission attempts % for IC, CC, EC channels during unexpected fading.

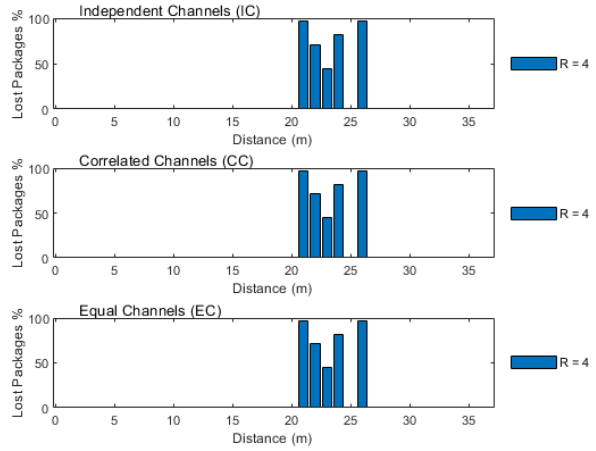

FIGURE 10. Rejected packets after last retransmission R = 4.

As we can see, all of the blocks that were broadcast at a distance of 21m were retransmitted four times in total. The identical thing happens at a distance of 26 meters. The blocks were retransmitted roughly 50% of the time along the other distances. If a block is refused, the algorithm recovers it by adding up all of the retransmission energy it has received. We saw that the performance related to the transmission attempts is similar for each of the channels. Only the correlated channel transmitted fewer packets during retransmission compared to others.

Figure 10 presents the number of rejected packets after the fourth attempt for each channel (IC, CC, EC) during fading. Here, we observed that all channels lost most of the blocks after four retransmissions. This limitation is related to the maximum gain provided by the transmitter and the channel condition in the previous retransmissions.

Figure 11 illustrates delay versus SNR between the first and the transmission and the final transmission required to achieve optimal power for each channel (IC, CC, EC). We see

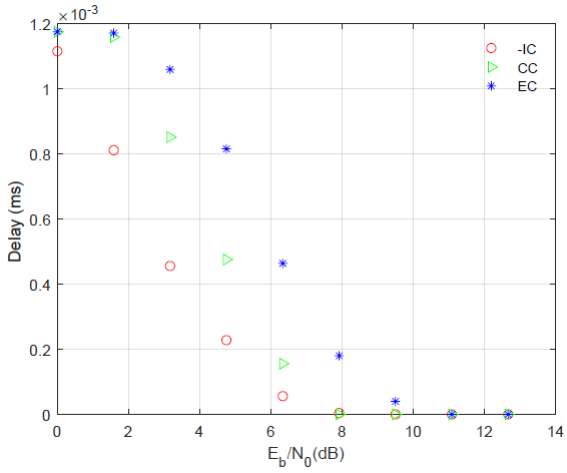

FIGURE 11. Delay between transmitted and received blocks for IC, CC, EC channels R = 4, distance = 50m.

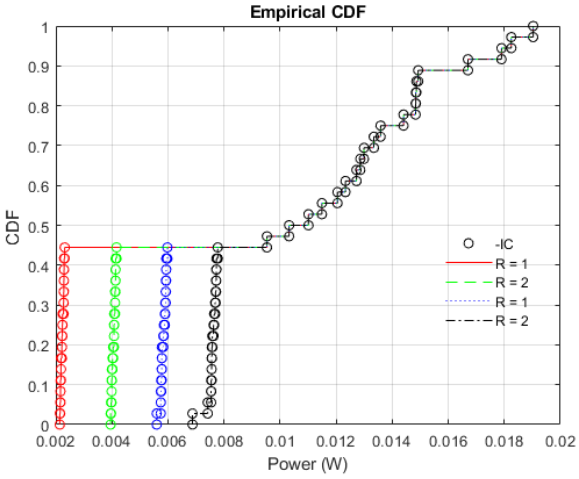

FIGURE 12. CDF received power among retransmissions for IC, CC, EC channels R = 4, distance = 50m.

that the retransmission attempt adds an additional delay to the system for all channels. Also, the delay is reduced as the SNR rises for all channels

Figure 12 demonstrates the CDF versus power for IC channel. When the channel experiences fading, the power is adjusted in each transmission attempt in order for the loss of the signal strength. If no losses occur, the power level remains the same (with no adjustments).

B. NON-LINEAR EQUALIZATION WITH AND WITHOUT CONSTANT POWER ADAPTATION

Figure 13 presents the received power over distance using constant adaptation. In this figure, the fading experienced by the drone is overcome by the retransmission attempt. The number of retransmissions is reduced to only one after the abrupt fading.

Figure 14(a) and 14(b) depict BER results when $Iter = 5$ and ϕ_k^R are 1 and 5. When $\phi_k^R = 1$, it means that the adaptive

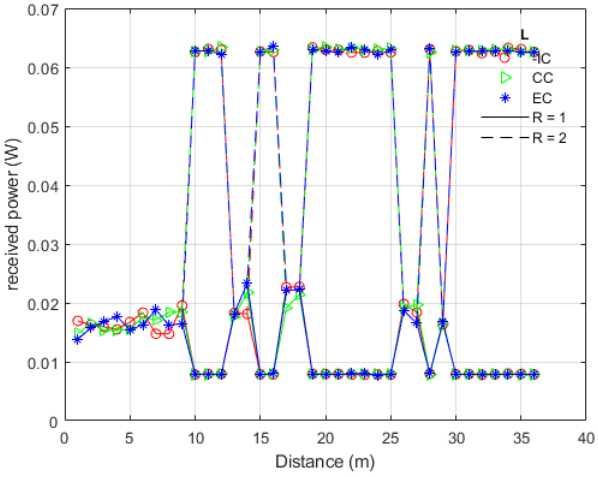

FIGURE 13. Power constant adaptation, $\phi_k^R = 4$. $Iter = 5$.

parameter and fading have the same value. This parameter was used to generate the BER in figure 14(a). In this case, the system relied on the IB-DFE iteration mechanism and the energy summation between blocks to recover from fading.

The first attempt achieved a $BER < 10^{-3}$ when the SNR was between 20 and 25 dB in all channels. In the second transmission, the SNR for all channels improved by at least 3dB. The independent channels improved the most significantly, from approximately 27 to 18 dB. The gain between retransmissions occured because IB-DFE reduced the ISI between the received symbols throughout each iteration, and the unsuccessful energy of blocks was added to the retransmitted ones. On the other hand, the second retransmission achieved a $BER = 10^{-3}$ when the SNR ranged from 3 to 11 dB for all of the channels when ϕ_k^R was five times greater than the fading experienced by the drone.

Figure 15 depicts the PER vs the normalized SNR Eb/N_0 per retransmission attempt (R1, R2) for each channel (IC, CC, EC) when distance = 50m, $Iter = 5$,and ϕ_k^R is 1 in figure 15 (a) and 5 in figure 15 (b).

Figure 16 (a), (b), (c) and (d) show the effects on PER after increasing the Adaptive factor proportionally in each simulation (i.e $\phi_k^R = 1, 2, 4, 10$, respectively). As we increased the power in the system, we saw that the PER results improved for all channels.

When $\phi_k^R > 1$, the number of retransmission attempts necessary were lowered to just one. However, power was squandered since it was raised needlessly in order to adjust the retransmission energy. There were no outages in this situation.

C. NON-LINEAR EQUALIZATION WITH POWER ADAPTATION

Previous results employed a constant ϕ_k^R across all retransmission attempts. With the help of APC, we demonstrate the effect of channel power variations across a range of distances in this section. As shown in equation (6),

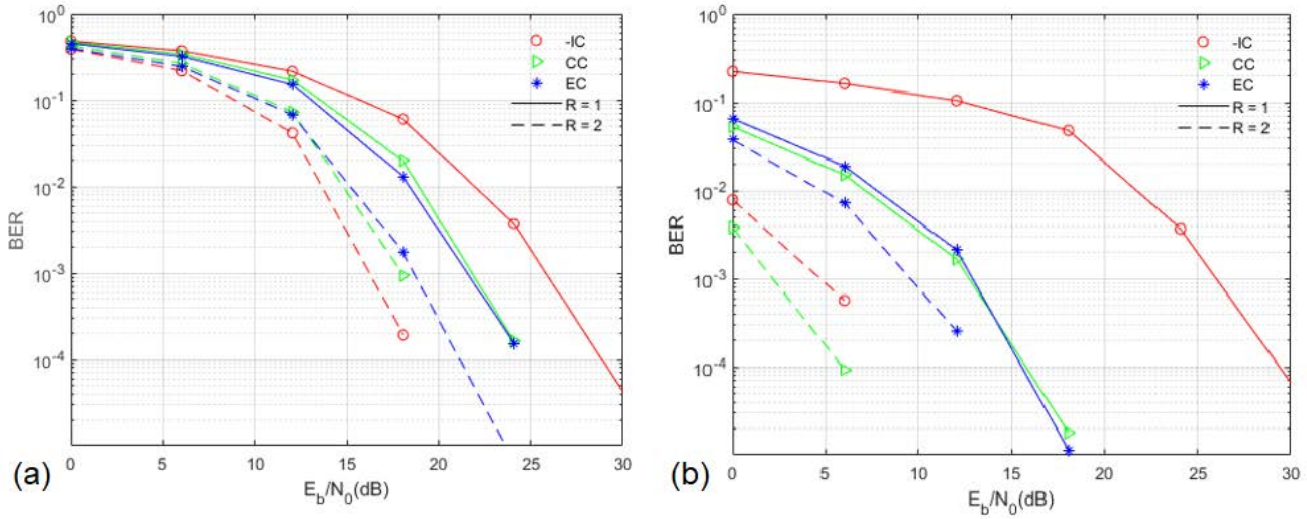

FIGURE 14. BER parameter for each retransmission attempt: distance = 50m, *Iter* = 5, (a): $\phi_k^R = 1$, (b): $\phi_k^R = 5$.

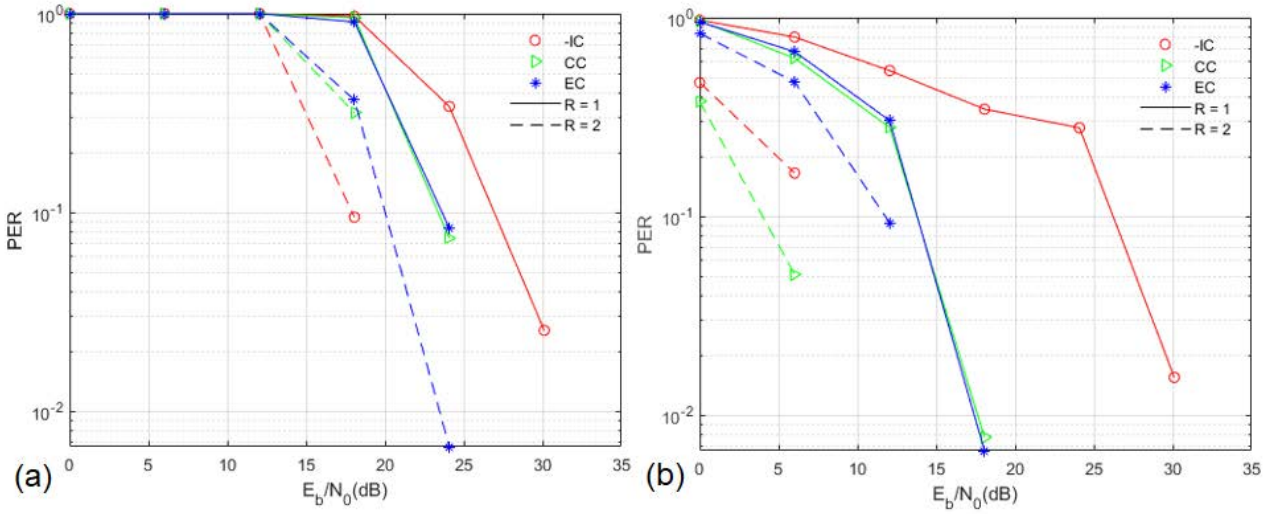

FIGURE 15. PER parameters for each retransmission attempt: distance = 50m, *Iter* = 5, (a): $\phi_k^R = 1$, (b): $\phi_k^R = 5$.

the variable ϕ_k^R is computed in real-time and changed in response to the decreasing power in the channel. Its value is updated to assure effective transmission based on prior experience.

For instance, using $10 - 3$W channel power, the drone effectively sent packets during previous fading circumstances. In order to replicate this successful experience, we adjusted our system such that it could provide the necessary power using the channel parameter. The values previously estimated in the receiver are sent back to the transmitter throughout NACK packets. After receiving NACK information, the transmitter adjusts the power to ensure the subsequent successful transmission. In this way, it was possible to optimize power usage until we achieved the maximum power available for communication in the UAV and reduced the number of retransmissions required.

Figure 17 depicts power over distance using the channel adaptation technique. While a usual telecommunication system requires B = K blocks to recover from attenuation of K. In this figure, we see that only one retransmission is needed to overcome fading for all channels used. In UAV scenarios, power is a constraint; consequently, such mechanisms are helpful to recover from packet loss. They are power efficient as they adapt the required power according to the environment using the information available in the NACK and retransmission packets.

Figure 18 presents the results related to BER when *Iter* = 5. We can achieve a $BER = 10^{-4}$ when SNR was approximately 25dB.

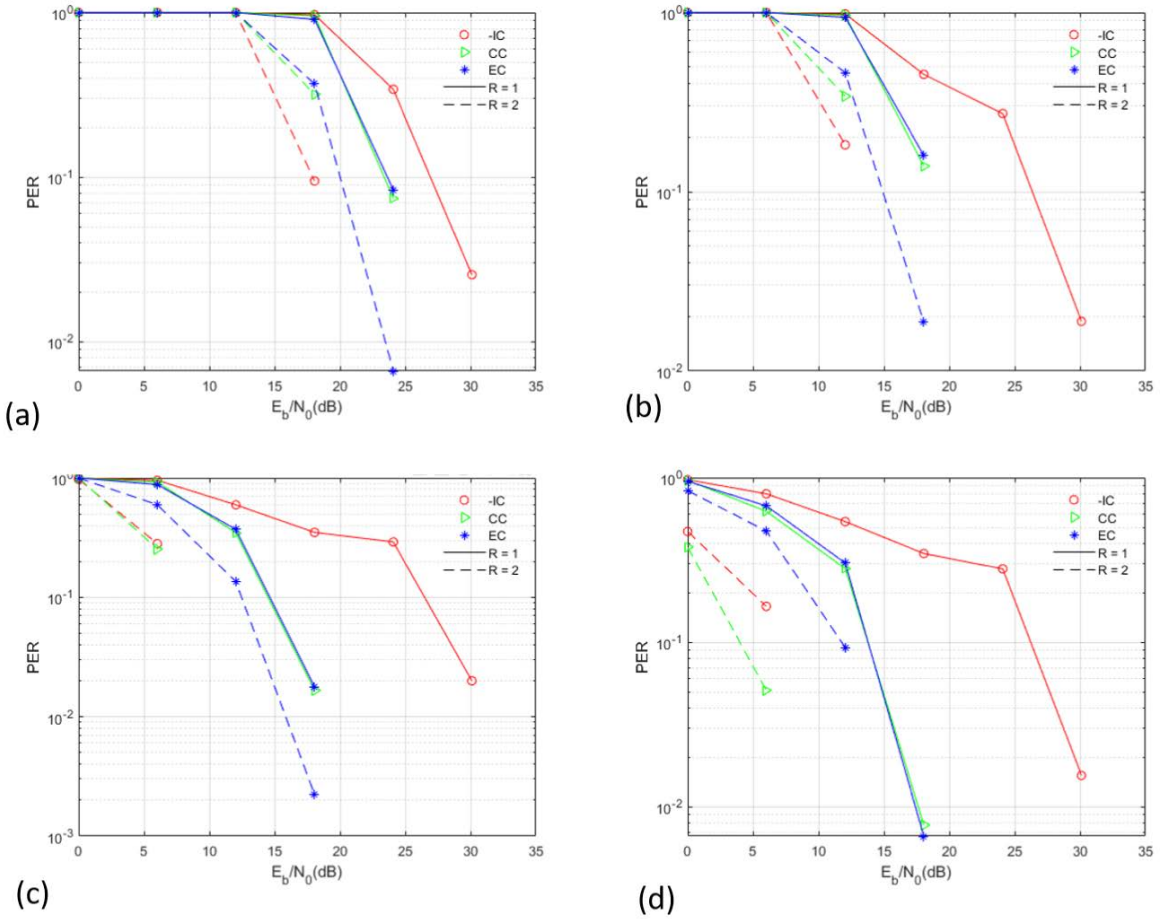

FIGURE 16. Recovered signal after adaptive packet combining in the retransmissions attempts.

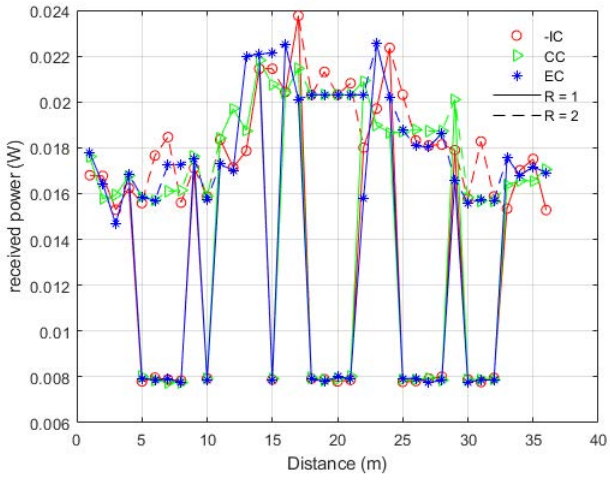

FIGURE 17. Power adaptation for all channels (IC, CC, EC), *Iter* = 5.

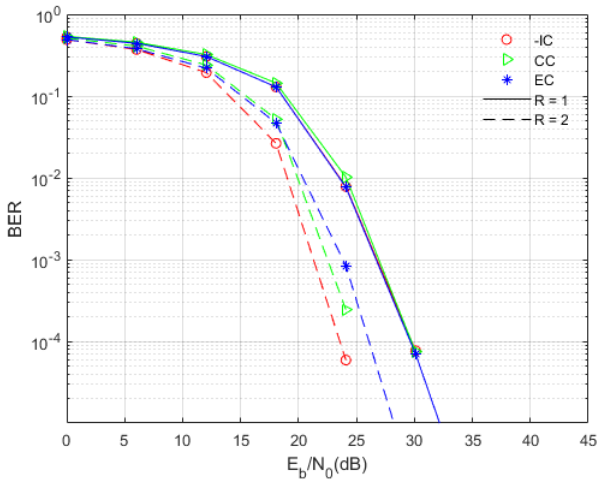

FIGURE 18. BER - IC, CC, EC channels using power adaptation, *Iter* = 5.

The corresponding results related to the retransmission amounts required to send a block successfully in CPC were seen in APC. It was possible to reduce the blocks retransmistted to only one or two depending on the interference and noise levels experienced by the drone. There were no outages and the drone used optimal adaptive communication power according to the changes in the environment.

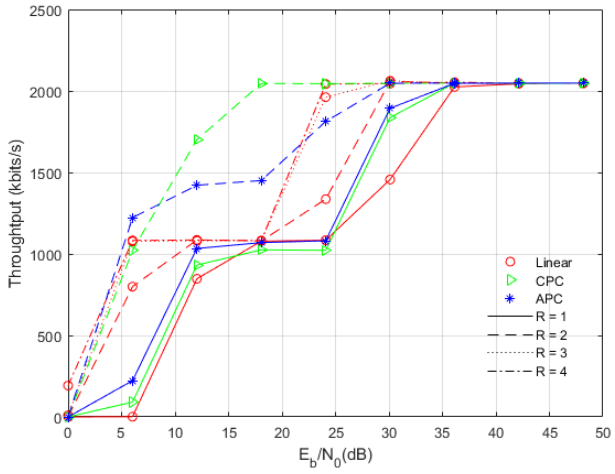

FIGURE 19. Throughput for independent channel using Linear: $Iter = 1$, $\phi_k^R = 1$, CPC: $Iter = 5$, $\phi_k^R = 6$, and APC: $Iter = 5$ methods.

The figure 19 highlights the achieved throughput using linear, CPC and APC techniques. According to the figure we see that the overall throughput rises when using CPC and APC with lower retransmission amounts resulting in an improvement in the system's reliability.

The validation of the results is based in the random environment obstruction not only in the small fading parameter.

V. CONCLUSION

Fading channels affect the overall transmitted information in the UAV A2G links, resulting in disconnection and restricting drones' ability to operate in LoS scenarios. We demonstrate that utilizing a linear adaptation to retransmit packets when the drone undergoes fading might boost the chances of successful packet reception. For instance, after four retransmission attempts, the overall power during the fading increased four times. The results for non-linear equalization with constant adaptation - CPC for BER and PER are satisfying. It is possible to reduce the number of transmissions to only one, but the power optimization is inadequate. With channel adaptation APC, on the other hand, there is no power dissipation, and the number of retransmissions per block stays at one. Additionally, Independent channels also provide considerable advantages over SNR ranges and retransmission attempts, as previously mentioned, this means that correct adjustment of the coherence time by the communication system might increase the results of our system. Finally, APC is an alternative to improve communication when the drone is confronted with natural and human-made obstacles and obstructions.

REFERENCES

[1] W. Jin, J. Yang, Y. Fang, and W. Feng, "Research on application and deployment of UAV in emergency response," in *Proc. IEEE 10th Int. Conf. Electron. Inf. Emergency Commun. (ICEIEC)*, Jul. 2020, pp. 277–280, doi: 10.1109/ICEIEC49280.2020.9152338.

[2] O. Bekkouche, K. Samdanis, M. Bagaa, and T. Taleb, "A service-based architecture for enabling UAV enhanced network services," *IEEE Netw.*, vol. 34, no. 4, pp. 328–335, Jul. 2020, doi: 10.1109/MNET.001.1900556.

[3] Z. Kaleem, M. Yousaf, A. Qamar, A. Ahmad, T. Q. Duong, W. Choi, and A. Jamalipour, "UAV-empowered disaster-resilient edge architecture for delay-sensitive communication," 2018, *arXiv:1809.09617*.

[4] W. Saad, M. Bennis, M. Mozaffari, and X. Lin, *Wireless Communications and Networking for Unmanned Aerial Vehicles*. Cambridge, U.K.: Cambridge Univ. Press, 2020, doi: 10.1017/9781108691017.

[5] Y. Zeng, I. Guvenc, R. Zhang, G. Geraci, and D. Matolak, *UAV Communications for 5G and Beyond* Hoboken, NJ, USA: Wiley, 2020. [Online]. Available: https://books.google.pt/books?id=FQULEAAAQBAJ

[6] H. C. Nguyen, R. Amorim, J. Wigard, I. Z. Kovács, T. B. Sørensen, and P. E. Mogensen, "How to ensure reliable connectivity for aerial vehicles over cellular networks," *IEEE Access*, vol. 6, pp. 12304–12317, 2018, doi: 10.1109/ACCESS.2018.2808998.

[7] M.-M. Zhao, Q. Shi, and M.-J. Zhao, "Efficiency maximization for UAV-enabled mobile relaying systems with laser charging," *IEEE Trans. Wireless Commun.*, vol. 19, no. 5, pp. 3257–3272, May 2020, doi: 10.1109/TWC.2020.2971987.

[8] W. Chen, J. Liu, H. Guo, and N. Kato, "Toward robust and intelligent drone swarm: Challenges and future directions," *IEEE Network*, vol. 34, no. 4, pp. 278–283, Jul./Aug. 2020, doi: 10.1109/MNET.001.1900521.

[9] C. She, C. Liu, T. Q. S. Quek, C. Yang, and Y. Li, "Ultra-reliable and low-latency communications in unmanned aerial vehicle communication systems," *IEEE Trans. Commun.*, vol. 67, no. 5, pp. 3768–3781, May 2019, doi: 10.1109/TCOMM.2019.2896184.

[10] A. Abdrabou, B. Liang, and W. Zhuang, "Delay analysis for sparse vehicular sensor networks with reliability considerations," *IEEE Trans. Wireless Commun.*, vol. 12, no. 9, pp. 4402–4413, Sep. 2013, doi: 10.1109/TW.2013.072313.121397.

[11] M. M. Azari, F. Rosas, K.-C. Chen, and S. Pollin, "Ultra reliable UAV communication using altitude and cooperation diversity," *IEEE Trans. Commun.*, vol. 66, no. 1, pp. 330–344, Jan. 2018, doi: 10.1109/TCOMM.2017.2746105.

[12] Y. Han, L. Liu, L. Duan, and R. Zhang, "Towards reliable UAV swarm communication in D2D-enhanced cellular networks," *IEEE Trans. Wireless Commun.*, vol. 20, no. 3, pp. 1567–1581, Mar. 2021, doi: 10.1109/TWC.2020.3034457.

[13] I. Donevski, C. Raffelsberger, M. Sende, A. Fakhreddine, and J. J. Nielsen, "An experimental analysis on drone-mounted access points for improved latency-reliability," in *Proc. 7th Workshop Micro Aerial Vehicle Netw., Syst., Appl.*, Jun. 2021, pp. 31–36, doi: 10.1145/3469259.3470489.

[14] T. Shafique, H. Tabassum, and E. Hossain, "End-to-End energy-efficiency and reliability of UAV-assisted wireless data ferrying," *IEEE Trans. Commun.*, vol. 68, no. 3, pp. 1822–1837, Mar. 2020, doi: 10.1109/TCOMM.2019.2958805.

[15] P. S. Bithas, V. Nikolaidis, A. G. Kanatas, and G. K. Karagiannidis, "UAV-to-ground communications: Channel modeling and UAV selection," *IEEE Trans. Commun.*, vol. 68, no. 8, pp. 5135–5144, Aug. 2020, doi: 10.1109/tcomm.2020.2992040.

[16] V. Vahidi and E. Saberinia, "A low complexity and bandwidth efficient procedure for OFDM data reconstruction in DSC 5G networks," in *Proc. 15th IEEE Annu. Consum. Commun. Netw. Conf. (CCNC)*, Jan. 2018, pp. 1–4, doi: 10.1109/CCNC.2018.8319266.

[17] S. Kumari, K. K. Srinivas, and P. Kumar, "Channel and carrier frequency offset equalization for OFDM based UAV communications using deep learning," *IEEE Commun. Lett.*, vol. 25, no. 3, pp. 850–853, Mar. 2021, doi: 10.1109/LCOMM.2020.3036493.

[18] B. Ji, Y. Li, B. Zhou, C. Li, K. Song, and H. Wen, "Performance analysis of UAV relay assisted IoT communication network enhanced with energy harvesting," *IEEE Access*, vol. 7, pp. 38738–38747, 2019, doi: 10.1109/ACCESS.2019.2906088.

[19] A. A. Khuwaja, Y. Chen, and G. Zheng, "Effect of user mobility and channel fading on the outage performance of UAV communications," *IEEE Wireless Commun. Lett.*, vol. 9, no. 3, pp. 367–370, Mar. 2020, doi: 10.1109/LWC.2019.2955444.

[20] T. Z. H. Ernest, A. S Madhukumar, R. P. Sirigina, and A. K. Krishna, "NOMA-aided UAV communications over correlated rician shadowed fading channels," *IEEE Trans. Signal Process.*, vol. 68, pp. 3103–3116, 2020, doi: 10.1109/TSP.2020.2994781.

[21] C. You and R. Zhang, "3D trajectory optimization in Rician fading for UAV-enabled data harvesting," *IEEE Trans. Wireless Commun.*, vol. 18, no. 6, pp. 3192–3207, Jun. 2019, doi: 10.1109/TWC.2019.2911939.

[22] Z. Cui, C. Briso-Rodriguez, K. Guan, Z. Zhong, and F. Quitin, "Multi-frequency air-to-ground channel measurements and analysis for UAV communication systems," *IEEE Access*, vol. 8, pp. 110565–110574, 2020, doi: 10.1109/ACCESS.2020.2999659.
[23] T. Liu, Z. Zhang, H. Jiang, Y. Qian, K. Liu, J. Dang, and L. Wu, "Measurement-based characterization and modeling for low-altitude UAV air-to-air channels," *IEEE Access*, vol. 7, pp. 98832–98840, 2019, doi: 10.1109/ACCESS.2019.2929955.
[24] J. Liu, H. Zhang, M. Sheng, Y. Su, S. Chen, and J. Li, "High altitude air-to-ground channel modeling for fixed-wing UAV mounted aerial base stations," *IEEE Wireless Commun. Lett.*, vol. 10, no. 2, pp. 330–334, Feb. 2021, doi: 10.1109/LWC.2020.3029824.
[25] X. Wang, W. Feng, Y. Chen, and N. Ge, "Coverage optimization for UAV-aided Internet of Things with partial channel knowledge," *J. Commun. Inf. Netw.*, vol. 3, no. 4, pp. 55–63, Dec. 2018, doi: 10.1007/s41650-018-0039-9.
[26] M. Pereira, R. Dinis, L. Bernardo, R. Oliveira, and P. Pinto, "Frequency-domain cross-layer diversity techniques: An efficient way of coping with lost packets in broadband wireless systems," *IEEE Wireless Commun.*, vol. 20, no. 5, pp. 100–108, Oct. 2013, doi: 10.1109/MWC.2013.6664480.
[27] M. R. Pereira, "Time diversity solutions to cope with lost packets," Ph.D. dissertation, Faculdade de Ciências e Tecnologia, Almada, Portugal, 2013. [Online]. Available: https://core.ac.U.K./display/157626204
[28] F. C. Ribeiro, J. Guerreiro, R. Dinis, F. Cercas, A. Silva, and A. N. Pinto, "Nonlinear effects of radio over fiber transmission in base station cooperation systems," in *Proc. IEEE Globecom Workshops (GC Wkshps)*, Dec. 2017, pp. 1–6, doi: 10.1109/GLOCOMW.2017.8269172.
[29] F. C. Ribeiro, J. Guerreiro, R. Dinis, F. Cercas, and A. Silva, "Reduced complexity detection in MIMO systems with SC-FDE modulations and iterative DFE receivers," *J. Sensor Actuator Netw.*, vol. 7, no. 2, p. 17, Apr. 2018, doi: 10.3390/jsan7020017.

JOSEANNE VIANA (Member, IEEE) received the bachelor's degree in telecommunication engineering from the University of Campinas, Brazil. She is currently pursuing the Ph.D. degree with the ISCTE–Lisbon University Institute in the Radio Systems Department. She is an Early-Stage Researcher in the project TeamUp5G, a European Training Network in the frame of (MSCA ITN) of the European Commission's Horizon 2020. Her research interests include wireless communications applied to interconnected systems, such as UAVs, aerial vehicles, and non-terrestrial devices.

JOÃO MADEIRA received the master's degree in electrical engineering and computer science from the Nova School of Science and Technology, Lisbon, where he is currently pursuing the Ph.D. degree. He has worked in research and development with technological startups in several European research projects involving UAVs and secure wireless communications. His research interests include high efficiency wireless transmission, software-defined radios, and forward error correction.

NIDHI (Member, IEEE) received the bachelor's degree in electronics and telecommunication and the masters' degree in electronics and communication (wireless) from India. She is currently pursuing the Ph.D. degree with the Department of Business Development and Technology, Aarhus University. She is also an Early-Stage Researcher in the project TeamUp5G, a European Training Network in the frame of (MSCA ITN) of the European Commission's Horizon 2020 framework. Her research interests include small cells, spectrum management, and carrier aggregation.

PEDRO SEBASTIÃO (Member, IEEE) received the Ph.D. degree in electrical and computer engineering from IST. He is currently a Professor with the ISCTE-IUL's Information Science and Technology Department. He is also the Board Director of the AUDAX-ISCTE-Entrepreneurship and Innovation Center, ISCTE, responsible for the LABS LISBOA Incubator and a Researcher at the Instituto de Telecomunicações. He has oriented several master's dissertations and doctoral theses. He has been responsible for several national and international research and development projects. He has been an expert and evaluator of more than one hundred national and international civil and defense research and development projects. It has several scientific, engineering, and pedagogical awards. He has organized or co-organized more than 55 national and international scientific conferences. He planned and developed several postgraduate courses in technologies and management, entrepreneurship and innovation, and transfer of technology and innovation. He has supported several projects involving technology transfer and creation of start-ups and spinoffs of value to society and market. He developed his professional activity in the National Defense Industries, initially in the Office of Studies and later as the Board Director of the Quality Department of the Production of New Products and Technologies. He was also responsible for systems of communications technology in the Nokia-Siemens business area. He is the author or coauthor of more than 200 scientific articles. His main research interests include monitoring, control, and communications of drones, unmanned vehicles, planning tools, stochastic process (modeling and efficient simulations), the Internet of Things, and efficient communication systems.

FRANCISCO CERCAS (Senior Member, IEEE) has more than 38 years of professional experience, including teaching at High School and Industry as a Research Engineer (CENTREL EID 1982–1983) before entering the academic career in 1984. He was the President of his Department (DCTI 2007–2010), the School Dean (ISTA 2010–2013), and the President of the University's Scientific Council (ISCTE-IUL 2015–2018). He was a Lecturer at the Instituto Superior Técnico (IST), Lisbon, during 15 years, then at ISCTE-IUL, where he is a Full Professor, since 2012. He is or was a Researcher at the Satellite Centre, CAPS, INESC, University of Plymouth, U.K., and the Instituto de Telecomunicações (IT), where he leads of the Radio Group IT-IUL. He has been a National Coordinator of telecommunications at Ordem dos Engenheiros, since 2014. He has supervised seven Ph.D. completed theses, as well as many M.S.C. and Final Year's Projects at both IST and ISCTE-IUL. He participated in several national and international projects. He was National Delegate of four COST European projects. He is the coauthor of a new class of codes named Tomlinson, Cercas, Hughes (TCH) and more than 200 publications, including one patent, four book chapters, 25 journal articles, more than 150 conference papers, and several international research reports. His research interests include satellite and mobile communications, coding theory, and spread spectrum communications and related topics.

ALBENA MIHOVSKA (Member, IEEE) received the Ph.D. degree in mobile communications from Aalborg University, Denmark. Since 2017, she has been an Associate Professor with the Department of Business Development and Technology, Aarhus University, Denmark, where she is leading the research activities of the 6G Knowledge Laboratory, with a focus on 6G connectivity and enabling technologies, namely artificial intelligence, and advanced services and applications, such as augmented and extended reality (AR and XR), high-fidelity and real time mobile hologram, and digital twins. She is currently a Senior Research and an Academic Professional. She has more than 150 scientific publications.

RUI DINIS (Senior Member, IEEE) received the Ph.D. degree from the Instituto Superior Técnico (IST), Technical University of Lisbon, Portugal, in 2001, and the Habilitation degree in telecommunications from the Faculdade de Ciências e Tecnologia (FCT), Universidade Nova de Lisboa (UNL), in 2010. He was a Researcher with the Centro de Análise e Processamento de Sinal (CAPS), IST, from 1992 to 2005, and the Instituto de Sistemas e Robótica (ISR), from 2005 to 2008. From 2001 to 2008, he was a Professor at IST. In 2003, he was an Invited Professor with Carleton University, Ottawa, ON, Canada. Since 2009, he has been a Researcher with the Instituto de Telecomunicações (IT). He is currently an Associate Professor with FCT, Universidade Nova de Lisboa (UNL). He has been actively involved in several national and international research projects in the broadband wireless communications area. His research interests include transmission, estimation, and detection techniques. He was/is an Editor of the IEEE TRANSACTIONS ON WIRELESS COMMUNICATIONS, the IEEE TRANSACTIONS ON COMMUNICATIONS, the IEEE TRANSACTIONS ON VEHICULAR TECHNOLOGY, the IEEE OPEN JOURNAL OF THE COMMUNICATIONS SOCIETY, and *Physical Communication* (Elsevier). He was also a Guest Editor of *Physical Communication* (Elsevier) (Special Issue on Broad- band Single-Carrier Transmission Techniques). He is a VTS Distinguished Lecturer.